Electrochimica Acta 215 (2016) 420–426

Contents lists available at ScienceDirect

Electrochimica Acta

journal homepage: www.elsevier.com/locate/electacta

Highly active and selective nickel molybdenum catalysts for direct hydrazine fuel cell

Tristan Asset[a,b], Aaron Roy[c], Tomokazu Sakamoto[d], Monica Padilla[c], Ivana Matanovic[c,f], Kateryna Artyushkova[c], Alexey Serov[c], Frederic Maillard[a,b], Marian Chatenet[a,b,g,*], Koichiro Asazawa[d], Hirohisa Tanaka[d,e], Plamen Atanassov[c,*]

[a] Univ. Grenoble Alpes, LEPMI, F-38000 Grenoble, France
[b] CNRS, LEPMI, F-38000 Grenoble, France
[c] Chemical & Biological Engineering Department, UNM Center for Micro-Engineered Materials, University of New Mexico, Albuquerque, NM 87131, USA
[d] Advanced R&D Dept., R&D Center, Corporate Business Unit, Daihatsu Motor Co., Ltd.,3000, Yamanoue, Ryuo, Shiga 520-2593, Japan
[e] Currently with the Department of Nanotechnology for Sustainable Energy, School of Science and Technology, Kwansei Gakuin University, 2-1 Gakuen, Sanda, Hyogo 669-1337, Japan
[f] Theoretical Division, Los Alamos National Laboratory, Los Alamos, NM 87545, USA
[g] French University Institute, IUF, Paris, France

ARTICLE INFO

Article history:
Received 9 May 2016
Received in revised form 22 August 2016
Accepted 22 August 2016
Available online 24 August 2016

Keywords:
Direct Hydrazine Fuel Cell
Ni-based catalyst
Nickel
Molybdenum
Ammonia Generation

ABSTRACT

Carbon-supported NiMo catalysts (NiMo/C) were synthesized and investigated for the electrooxidation of hydrazine. Their morphology and composition were determined with physicochemical characterizations (TEM-EDS, XPS and XRD) and further bridged to their electrocatalytic activity. The electrochemical performances measured in rotating disk electrode experiments reached 7.68 ± 0.96 kA g_{metal}^{-1} for hydrazine electrooxidation at $E = 0.4$ V *vs.* RHE for the carbon-supported NiMo (9:1)/C. This value is amongst the highest reported in the literature. The large activity of the carbon-supported NiMo (9:1)/C catalyst was ascribed to the effect of a low but non-negligible (<15 at. %) molybdenum content, as molybdenum atoms stabilize the hydrazine N-N bond, thereby preventing the chemical decomposition of hydrazine into ammonia, and improving the catalyst selectivity towards the complete (and desired) hydrazine oxidation into N_2 gas.

1. Introduction

The interest for fuel cells has been growing over the past decades, as a response to the forecast depletion of fossil energies. Indeed, fuel cells enable a more efficient fuel-to-electricity conversion than internal combustion engines. In particular, low-temperature fuel cells are extremely promising technologies for a wide range of applications, such as portables electronic devices, electric vehicles, or stationary power supplies. However, they must overcome several challenges to become commercially viable. For example, the development of proton exchange membrane fuel cells (PEMFCs) and direct alcohol fuel cells (DAFCs) presents issues linked to the anodic and cathodic electrocatalysts. Their catalysts materials are typically based on Pd and Pt [1,2], which implies cost and availability issues. Reducing the noble metal content in fuel cells is mandatory, and this can be achieved by *(i)* using tailored nanostructured materials, such as core-shell or alloy solid/hollow nanoparticles [3–8], or by *(ii)* focusing on non-noble materials. In that latter strategy, recent but nonetheless impressive progresses have been obtained with catalysts of the carbon-nitrogen-iron family for the oxygen reduction reaction (both in alkaline and acidic conditions) [9–12].

On the anode side, the most studied fuels to feed these systems still present drawbacks: hydrogen gas is expensive to produce in a sufficiently clean manner, to store/transport, and there are still no active noble-free catalysts capable to oxidize hydrogen efficiently. Oxygenated organic molecules (alcohols, aldehydes, organic acids, *etc.*) are easily produced, stored and transported, but their oxidation proceeds with very sluggish kinetics even on noble catalysts, adversely affecting the DAFC performances-to-catalyst

* Corresponding authors.
E-mail addresses: marian.chatenet@phelma.grenoble-inp.fr (M. Chatenet), plamen@unm.edu (P. Atanassov).

http://dx.doi.org/10.1016/j.electacta.2016.08.106
0013-4686/

cost ratio [1,2]. The choice of potential fuels is however wider in alkaline than in acidic medium, which enables to look at candidates beyond molecular hydrogen and the alcohols family. In particular, non-carbon fuels of the boron (*e.g.* $NaBH_4$, NH_3BH_3) and nitrogen-derived family (N_2H_4) are of interest, owing to their large theoretical energy density, ease of storage/transport and faster overall oxidation kinetics than for their carbon-containing competitors [13–20].

In particular, hydrazine oxidation as a replacement for alcohol or hydrogen oxidation was extensively studied from the sixties to nowadays [21–34].

$$\mathbf{N_2H_4 + 4OH^- \rightarrow N_2 + 4H_2O + 4e^-} \quad \boldsymbol{E^0 = -0.33 V vs. RHE} \qquad (1)$$

The DHFC (direct hydrazine fuel cell), which completes the oxygen reduction reaction at the cathode, also presents a higher theoretical cell voltage than PEMFC fed with hydrogen: 1.56 V *vs.* 1.23 V, owing to the very strong reducing behaviour of its fuel (Eq. (1)). Insuring DHFCs efficiency is essential to enable their commercialization; in that frame one should avoid the chemical decomposition of hydrazine into ammonia (NH_3, Eq. (2)), since it leads to incomplete fuel oxidation (lower faradic efficiency), poisoning of the anode catalyst by ammonia (and also of the cathode catalyst if ammonia cross-over proceeds through the membrane), all these phenomena decreasing the voltage and therefore the energy density of the DHFC [18].

$$N_2H_{4,ads} + 2H_2O \rightarrow 2OH_{ads} + 2NH_{3,ads} \qquad (2)$$

Sakamoto *et al.* [24,25,27] observed that alloying nickel with another metal (*e.g.* cobalt, lanthanum or zinc) improves the catalysts performances toward hydrazine oxidation, both in the rotating disk electrode (RDE) and membrane electrode assembly (MEA) configurations. For example, unsupported nickel nanoparticles in DHFC anodes combined with a Co-polypyrrole-catalyzed carbon cathode (Co-PPY-C) for the oxygen reduction reaction (ORR) presented a lower maximum power density (389 mW cm^{-2})[24] than unsupported Ni_1Co_1 (423 mW cm^{-2}), unsupported Ni_9La_1 (453 mW cm^{-2}) and unsupported $Ni_{0.87}Zn_{0.13}$ (elaborated by spray pyrolysis [26], 486 mW cm^{-2}) in identical operating conditions (T = 353 K, anolyte = 1 M KOH + 20% H_2O-N_2H_4). However, Daihatsu Motor Co. reported substantial ammonia production (from several hundred to several thousand ppm) on the catalysts listed above, which is unsuitable for widespread and durable DHFC applications [35]. Consequently, a major challenge for DHFC commercialization is to avoid hydrazine chemical decomposition without reducing the catalyst electrochemical performances (*i.e.* enable the selective and complete hydrazine oxidation of Eq. (1)). To this goal, one strategy is to investigate other elements that alloy with Ni. It has been shown that the presence of molybdenum in Ni-based catalyst influences their selectivity and efficiency toward several reactions [36,37]. Based on this, the present study focuses on the synthesis of Ni_xMo_y/C catalysts and the analysis of the effect of molybdenum on the catalyst morphology and electrochemical performances.

2. Experimental

2.1. Ni-Mo catalysts elaboration

The carbon-supported NiMo catalysts were synthesized using a wet impregnation procedure. Firstly, calculated amounts of molybdenum precursor (Aldrich, $(NH_4)_6Mo_7O_{24}{}^*4H_2O$), nickel precursor (Aldrich, $N_2NiO_6{}^*6H_2O$) and urea (Aldrich CN_2H_4O) were dissolved in ultrapure water, to obtain a specific nickel/molybdenum ratio. The theoretical ratios synthesized by the wet impregnation process were: NiMo (1:1); NiMo (2:1); NiMo (3:1); NiMo (4:1); NiMo (9:1) and Ni. Since urea was added to reduce the molybdenum precursor, no urea was added during the synthesis of the pure nickel catalyst. A calculated amount of carbon (Akzo Nobel Ketjen Black EC-600 JD) was dissolved in H_2O + IPA (isopropyl alcohol), to obtain 50 wt. % metallic loading. The metal precursors and the carbon powder were then mixed and dispersed using an ultrasonic probe during 5 min., before overnight drying at T = 358 K. This step was followed by 1 h heat-treatment at T = 823 K under 7 at. % H_2 atmosphere (balanced with Ar), with a 15 K min^{-1} heating ramp, to complete the metal precursors reduction and eliminate their ligands. After cooling, the catalyst was passivated by flowing argon in the tube for 15 min, followed by t = 30 min under 3% O_2 flow.

2.2. Physicochemical characterizations

2.2.1. X-ray diffraction

Carbon-supported Ni and NiMo catalysts were analysed by X-ray diffraction (XRD) using a Scintag Pad V diffractometer (Bragg-Brentano geometry) with Data Scan 4 software (from MDI, Inc.) for system automation and data collection. Cu Kα radiation (40 kV, 35 mA) was used with a Bicron Scintillation detector (with a pyrolitic graphite curved crystal monochromator).

2.2.2. Transmission electron microscopy

Transmission electron microscopy (TEM) as well as energy dispersive spectrometry (X-EDS) were performed on a JEOL 2010 microscope, equipped with a LaB_6 filament and operated at 200 kV accelerating voltage (point-to-point resolution of 0.19 Å). The TEM micrographs were used to characterize the distribution of the metal nanoparticles on the carbon powder support and the particle sizes. The local or global Mo and Ni atomic percentages were determined by X-EDS using Oxford Inca control software. The acquisition was performed at the classical acceleration voltage of 200 kV on selected areas of the samples, over dozens (local analysis) to thousands (global analysis) of particles. The quantitative analyses were performed on Ni Kα and Mo Kα signal lines using the K factor provided by Oxford Inca software.

2.2.3. X-ray photoelectron spectroscopy

The X-ray photoelectron spectroscopy (XPS) analyses were performed using a Kratos AXIS-Ultra DLD photoelectron spectrometer using a monochromatic Al Kα source operating at P = 225 W. No charge compensation was necessary. The survey of the sample was done first, followed by the recording of high-resolution spectra of C 1s, O 1s, Ni 2p and Mo 3d for three areas on the sample. All spectra processing was done in CasaXPS. Atomic % were calculated using sensitivity factors provided by the

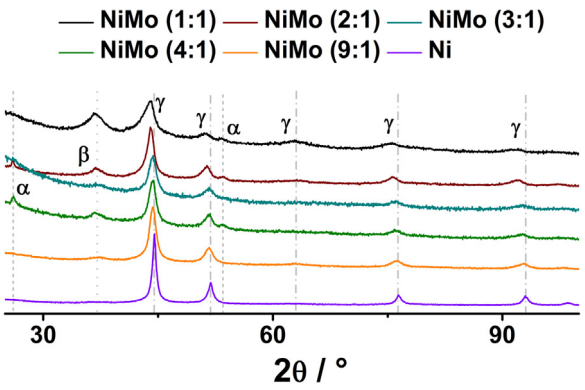

Fig. 1. XRD patterns of the NiMo/C electrocatalysts with the peaks for the (α) MoO_2, (β) $Ni_{0.16}Mo_{0.84}$ and (γ) $(Ni_9Mo)_{0.4}$.